CHEMISTRY
A European Journal

A Journal of
ChemPubSoc Europe

Accepted Article

Title: Mono-aryl/alkythio-substituted (Hetero)acenes of Exceptional Thermal and Photochemical Stability via Thio-Friedel Crafts/ Bradsher Cyclization Reaction

Authors: Piotr Balczewski, Emilia Kowalska, Joanna Skalik, Ewa Różycka-Sokołowska, Krzysztof Owsianik, Marek Koprowski, Bernard Marciniak, Dariusz Guziejewski, and Witold Ciesielski

To be cited as: *Chem. Eur. J.* 10.1002/chem.201903027

Link to VoR: http://dx.doi.org/10.1002/chem.201903027

Supported by
ACES

WILEY-VCH

Chemistry - A European Journal 10.1002/chem.201903027

FULL PAPER WILEY-VCH

Mono-aryl/alkylthio-substituted (Hetero)acenes of Exceptional Thermal and Photochemical Stability via Thio-Friedel Crafts/Bradsher Cyclization Reaction

Piotr Bałczewski,*[a, b] Emilia Kowalska,[a] Ewa Różycka-Sokołowska,[b] Joanna Skalik,[a] Krzysztof Owsianik,[a] Marek Koprowski,[a] Bernard Marciniak,[b] Dariusz Guziejewski,[c] Witold Ciesielski[c]

Abstract: Significantly substituted mono-aryl/alkylthio-(RS)-(hetero)acenes are thermally more stable ($T_{dec.}$= 331-354 °C) than known di-RS-substituted acenes by average 25 °C. They are also much more photostable at 254 and 365 nm (both in argon/air) than parent anthracene and other reported anthracenes. The most photostable RS-anthracenes (254 nm) were 60-70 (air) and 130 (argon) times more stable in solution than the unsubstituted anthracene and much more stable than known EDG/EWG - substituted anthracenes with extended aromatic core. The photostability significantly increased at 365 nm both in air and argon. The mono-RS-(hetero)acenes are blue light emitting fluorophores. They have been obtained in the novel thio-Friedel-Crafts/Bradsher cyclization reaction of unknown *ortho*-1,3-dithianylaryl(aryl)methyl thioethers. The developed approach gives a general access to mono-RS-(hetero)acene frameworks that may contain at least 3 or 4 fused (hetero)aromatic rings. The characteristic feature of this approach leading to significantly substituted acenes is that substituents, unlike in other methods, may be introduced at the early stage of the synthesis. DFT and TD-DFT calculations confirmed a stabilizing role of RS substituent in mono-RS-substituted anthracenes which are the most stable anthracenes up to date. Their high photostability is mainly due to the singlet oxygen quenching by acene and the acene S_1 state quenching by molecular oxygen.

Introduction

(Hetero)acenes, despite their excellent electronic performance, are usually poorly soluble in organic solvents, which limits their direct use and processing. A further limitation is instability of the conjugated π-system and its destruction upon contact with oxygen and light due to photooxidation of double bonds to endoperoxides.[1-4] Other possible reactions are thermal-[5,6] and photochemical dimerizations.[7-8] These degradative processes are especially intensive for acenes larger than pentacene that are less stable and decompose already in the presence of visible light and air. In case of applications of smaller anthracenes as semiconductors, the higher stability toward the degradative processes compensates the disadvantage of their lower charge carrier mobilities in comparison with the larger analogs.[9] High photochemical stability is an important property of all acene materials, especially those suitable for use in small molecule and polymeric solar cells.[10]

In the literature of this field, the photochemical stability from seconds to hours has been reported for various acenes, and it depended, primarily, on the acene structure, presence or absence of oxygen, water and adsorbents as well as on the volume of photon energy delivered to the sample by various light sources.[3, 11-24] For the acenes, exposed to the low energy light sources, an increase of their light resistance to days has been observed. The increase effect has also been achieved by using stable radicals and utilization of the radicals characteristics to scavenge the energy of the photoexcited state of acenes.[25] Finally, photostability of acenes has significantly been enhanced when the acene was produced in a polymeric matrix.[17]

Further important factor determining the photochemical stability of the fused aromatic materials is presence of water[10] and oxygen.[13,14,17,18,20,22,26] Acenes can react with oxygen via either electron transfer (Type-I) or energy transfer mechanisms (Type-II) and both types are believed to operate simultaneously, whenever the acene is excited by irradiation (*cf.* our investigations).[4,11] The oxidation process, as mentioned, primarily leads to endoperoxides which may reproduce acenes upon thermolysis or photolysis.[11,27] For some acenes, like anthracene, photodimerisation occurs in the presence of air, especially in dilute solutions, in competition with photooxidation, leading to the corresponding endoperoxide. However, continued irradiation of anthracene and the endoperoxide in solution ultimately leads to the corresponding dione.[13]

The photostability has also been tested under anaerobic conditions.[1,28] In these studies, photostability of acenes was

---

[a] Prof. P. Bałczewski, Dr. E. Kowalska, Dr. J. Skalik, Dr. K. Owsianik, Dr. M. Koprowski
Division of Organic Chemistry, Group of Functional Materials Synthesis
Centre of Molecular and Macromolecular Studies, Polish Academy of Sciences
Sienkiewicza 112, 90-363 Łódź (Poland)
E-mail: pbalczew@cbmm.lodz.pl
[b] Prof. P. Bałczewski, Dr. E. Różycka-Sokołowska, Dr. B. Marciniak
Faculty of Mathematics and Natural Sciences, Institute of Chemistry, Health and Food Sciences, Department of Material & Structural Chemistry
Jan Długosz University in Częstochowa
Armii Krajowej 13/15, 42-201 Częstochowa (Poland)
[c] Dr. D. Guziejewski, Prof. W. Ciesielski
Department of Inorganic and Analytical Chemistry
University of Łódź
Pomorska 163, 90-236 Łódź (Poland)

Supporting information for this article is given via a link at the end of the document.

monitored by 50% decay of absorbance[21] or fluorescene,[13,15] ^{1}H-NMR spectra[17] and use of the HPLC technique.[15]

Another factor determining acenes photostability is their chemical structure including a kind and a number of fused rings, a presence of ring heteroatoms, steric hindrance and electronic character of substituents. Thus, electron-withdrawing and alkyne substituents, which enhance photostability, usually lower the LUMO energy in acenes. The lower LUMO orbital makes photoinduced electron transfer from the excited acene to O_2 less energetically favorable and results in a reduced rate of photooxidation *via* the electron transfer to oxygen mechanism (Type I) as well as results in the acene low triplet energy, which prevents singlet oxygen sensitization (Type II).[3,28]

The suitable substituents to increase photostability, such as 2-silylethynyl,[29-31] 2-phenylethynyl,[32] 2-t-butylethynyl,[29] 2-phenylethenyl,[4] heteroaryl (2-thienyl),[9,33] trifluoromethyl,[34] (4-trifluoromethyl)phenyl,[9] pentafluorophenyl,[35] halo (Cl, Br, F),[23,34,36] cyano,[34] alkoxy,[37] and *o,o'*-dialkylphenyl,[38] may be introduced to acene using a variety of synthetic strategies.[30] The most impressive substituent effect was observed with alkylthio- and arylthio- substituted pentacenes that were considerably more resistant to photooxidation than all other pentacene derivatives tested.[23,38] Similarly, a combination of arylthio- and bulky *o,o'*-dialkylphenyl substituents, dramatically enhanced photooxidative resistance of heptacenes.[39] In fact, the sulfenylated acenes turned out to be considerably better than silylethynyl substituents at enhancing photooxidative resistance of larger acenes.[23,38]

A review of known RS-substituted acenes, such as anthracenes,[39,40] tetra-,[40] penta-,[23,40-42] hepta-[38] and nonacenes[43] revealed acenes with two (from anthracene to heptacene*, vide supra*), eight and ten (both for nonacene, *vide supra*) RS substituents. The RS-substituted acenes showed not only increased chemical[40] and photochemical stability[38] but also useful optoelectronic properties.[23,38,40,41,43-45]

The discussed role of RS-substituents in sulfenylated acenes shows that alkyl-S and aryl-S groups or their combinations with other substituents may be considered as alternative or complementary substituents to the mentioned silylethynyl, *o,o'*-dialkylphenyl, halo, cyano, alkoxy, (fluoro)alkyl/aryl or heteroaryl groups in the design of new optoeletronic materials. On the other hand, systematic investigations on stability and properties of the mono-RS-substituted (hetero)acenes have not been carried out, so far.

The synthesis of mono-RS-substituted acenes may be realized *via* their direct sulfenylation only in a limited number of positions or via step-by-step introduction of RS-groups in the desired positions and in the controlled manner. The latter method is helpful, especially in the syntheses of larger, less stable (hetero)acenes but it has not been applied to the synthesis of mono-RS-(hetero)acenes. The 1,4-quinone methodology combining the above two methodologies, turned out to be the most versatile, so far.[38,43] The direct synthesis of RS-substituted acenes is limited to smaller anthracenes only and may be realized *via* the following transformations: sulfenylation of the middle, the most reactive anthracene ring[46] the X/RS exchange reactions (X = OH,[47] OMe,[48,49] OAc,[44] Br,[50-54] Cl,[53] NO_2[55]); Br/RS double exchange in 9,10-dibromoanthracene,[52,56] alkylation of anthracenethiols[57] and bisanthryldisulfides,[58] arylation of anthracenethiols,[59] as well as conversions of anthraquinones,[44,55] anthrones[48,56,49,58,60] or dithioanthraquinones[61] leading to mono- or di-RS-substituted anthracenes.

The above synthetic review and mentioned benefits from the presence of RS-groups in acenes, show a need for elaboration of new synthetic methodologies based on the controlled introduction of RS-groups in the desired positions of acenes which would enable: 1) a general access to both mono-RS-acenes and mono-RS-heteroacenes, 2) an access to significantly substituted derivatives, and 3) an access to larger mono-RS-substituted derivatives containing mixed arene and heteroarene fused rings. In this work, we are proposing such a general approach to stable mono-RS-substituted (hetero)acenes **6** containing 3 or 4 fused rings with a potential to a further extension of (hetero)aromatic π-conjugated systems.

Results and Discussion

Synthesis of (hetero)acenes 6.

The new approach involves, as a key step, an electrophilic cyclization of nonconjugated precursors, i.e. *ortho*-dithioacetalaryl(aryl)methyl thioethers **5** to give (hetero)acenes **6** substituted by various RS-groups (R = Ph, $C_6H_4CH_2$, 4-MeO-C_6H_4, 2-Naphthyl, *n*-$C_{12}H_{25}$). They are precisely located at the newly formed benzene ring which is fused to two (hetero)aromatic moieties, derived from (hetero)aromatic aldehydes (Scheme 1). This synthetic concept is, in fact, a new thio-variant of the Friedel-Crafts/Bradsher reaction[62] involving sulfur rich reagents.[63]

Realization of our strategy started with protection of the aldehyde **1** using 1,3-propanedithiol in refluxing benzene to give the 1,3-dithiane **2** in 82% yield following the procedure of Takano et al.[64] Then, the Br/Li exchange reaction with *n*-BuLi in the latter and condensation of the resulting aryllithium with various (hetero)aromatic aldehydes **3a-g**, afforded *ortho*-1,3-dithianylaryl(aryl)methanols **4a-g** in good 52-72% yields (Scheme 1, Table 1).[64] Only three examples of the latter have been described in literature, based on this sequence, so far.[64,65] Next, the diarylmethanols **4a-g** were effectively transformed into unknown thioethers **5** with various aliphatic, benzyl and aryl thiols in ethyl acetate, in the presence of stoichiometric amount of *p*-TsOH·H_2O, at room temperature (Scheme 1, Table 2; Table S1, see SI). Although the crude thioethers **5** were formed in good yields, a significant loss of materials was observed during their purification with column chromatography over silica gel or preparative TLC. The thioethers **5** were also sensitive to chlorinated solvents ($CHCl_3$, CH_2Cl_2). In order to avoid the loss of materials during the silica gel purification, realization of the final step of the thio-Friedel-Crafts/Bradsher cyclization was carried out using crude **5** as substrates and the $FeCl_3$ (1.2 equiv.)/KI (1.2 equiv.) reagents system in refluxing EtOH. After 0.5-24 h, the mono-RS-substituted (hetero)acenes **6** were

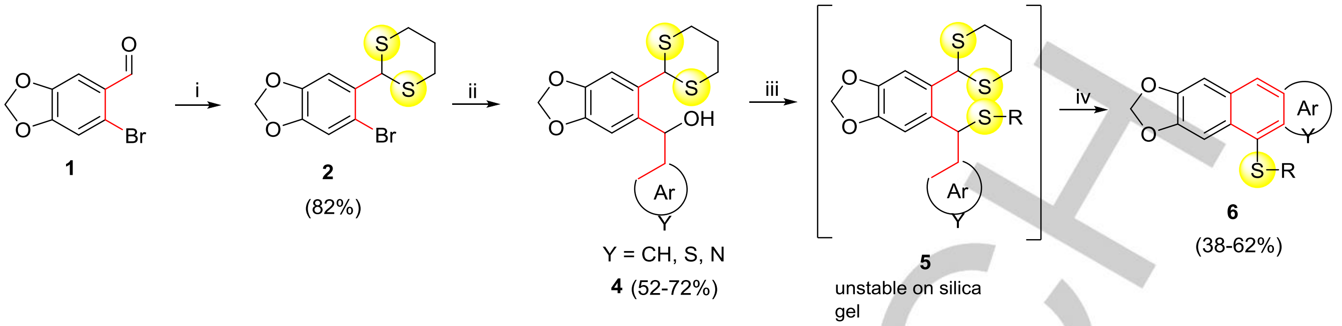

Reaction conditions: i) 1,3-propanedithiol, *p*-TsOH(cat.), benzene, reflux; ii) n-BuLi, aromatic aldehyde **3**, THF, -78°C; iii) *p*-TsOH, RSH, ethyl acetate, RT; iv) $FeCl_3$, KI, EtOH, reflux.

Scheme 1. Synthesis of mono-RS-substituted (hetero)acenes **6** from *ortho*-bromo substituted aromatic aldehydes **1**.

obtained in 38-62% and up to 43% total yields after two reaction steps (**4**→**5**→**6**), according to the analogous mechanism which was proposed by us for the oxygen version of the Friedel-Crafts/Bradsher cyclization reaction (for the mechanism of the sulfur variant, see SI).[66] It is worth mentioning that in some cases, when cyclization reactions were carried out in smaller scales, the products **5a, 5b** and **5d** precipitated after the standard work up procedure as white solids and they did not require a further purification. The crude products **6,** synthesized in bigger scales (>1.0 mmol), required purification with column chromatography over silica gel (Table 2). The thioethers **5a**, **5b, 5e-g** cyclized most effectively to give pure (hetero)acenes in good 50-62% yields (31-43% in the variant after two steps). The latter also precipitated from reaction mixtures and did not require further purification. The remaining thioethers **5c**, **5d** and **5h** cyclized to **6** less effectively (<46%) due to instability of the substrates **5** rather than products **6** under the reaction conditions. Cyclization of **5d** to 10-S-benzyl anthracene **6d** was accompanied by formation of the corresponding 10-ethoxy derivative (MS-EI, m/z = 356) which was formed in 11% yield, as a result of the S-CH_2Ph/OEt (from EtOH) group exchange, occurring *via* the corresponding intermediate dibenzylic carbocation.

In our further studies, we also considered an interesting approach to di-RS-substituted pentacenes **14** by a double thio-Friedel-Crafts/Bradsher cyclization of dithioethers **13** starting from 2,5-dibromobenzene-1,4-dicarbaldehyde **7** (Scheme 2). Thus, acetalization of the dialdehyde **7**[67] with 1,3-propanediol,[68] afforded the corresponding diacetal **8**[69] in excellent 99% yield. Next, bis(trans-thioacetalization)[70] of the latter with 1,3-propanedithiol gave the bis(dithioacetal) **9** also in 99% yield (Scheme 2). The direct bis(dithioacetalization) of the dialdehyde **7** with 1,3-propanedithiol failed. Surprisingly, lithiation of **9** with 2.2 equiv. of *n*-BuLi followed by condensation with 3,4,5-trimethoxybenzaldehyde afforded a mixture of mono- and bis(diarylmethanols) **10** and **12**, respectively in low 13% yields (Scheme 2). Optimization of the reaction conditions did not improve the yield of the desired diol **12**. Due to a low solubility of **12** in common organic solvents, the OH/SPh exchange could not be realized. On the other hand, the reaction of the diarylmethanol **10** with PhSH under standard acidic conditions (PhSH, *p*-TsOH, RT, AcOEt) gave only trace amounts of the desired product **11**. Introduction of longer alkyl chains in alkoxy groups should increase solubility of **12** and **13**.

Table 1. Synthesis of a series of *ortho*-1,3-dithianylaryl(aryl)methanols **4a-g**.

Aromatic aldehyde **3**	*ortho*-1,3-Dithianylaryl(aryl)methanol **4**	Yield [%][a]
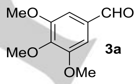 **3a**	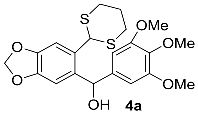 **4a**	52
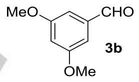 **3b**	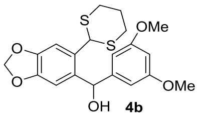 **4b**	55
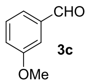 **3c**	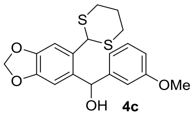 **4c**	68
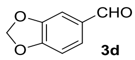 **3d**	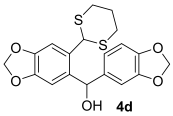 **4d**	72
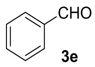 **3e**	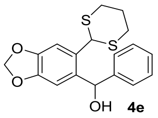 **4e**	62
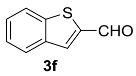 **3f**	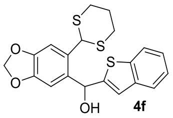 **4f**	66
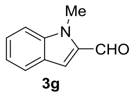 **3g**	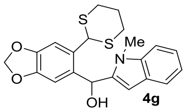 **4g**	45

[a] Yields of isolated products.

Table 2. *ortho*-1,3-Dithianylaryl(aryl)methyl thioethers **5** and (hetero)acenes **6**.

Alcohol **4**	RSH	Thioether **5**	Yield of **5** [%][a]/[%][b]	(Hetero)acene **6**	Reaction time	Yield of **6** [%][d]/[%][e]
4a	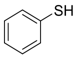	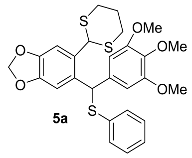 **5a**	51/73	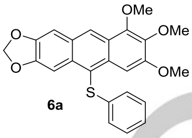 **6a**	30 min	62/43
4a	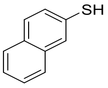	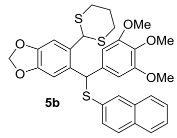 **5b**	42/71	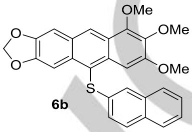 **6b**	30 min	51/42
4a	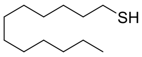	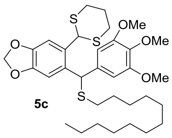 **5c**	45/-	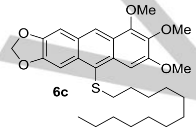 **6c**	45 min	46/8
4a	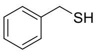	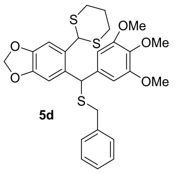 **5d**	28/51	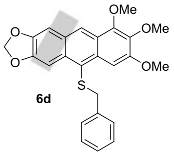 **6d**	45 min	38/6
4c	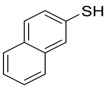	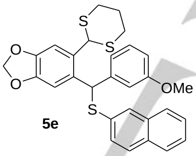 **5e**	32/-	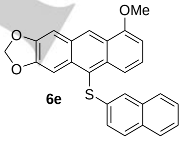 **6e**	90 min	50[d]/31[e]
4d	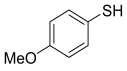	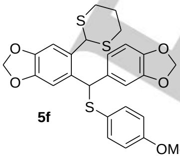 **5f**	28/-	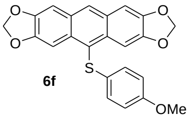 **6f**	60 min	52/15
4f	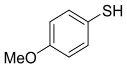	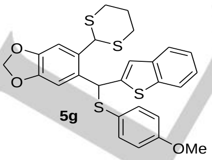 **5g**	54/-	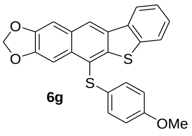 **6g**	60 min	57/32
4g	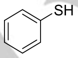	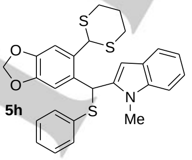 **5h**	-[c]	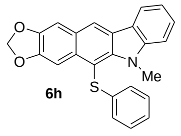 **6h**	24 h	-/7

[a] Yield of **5** after purification by column chromatography. [b] Yield of **5** after purification by precipitation. [c] Not isolated and directly subjected to the cyclization step. [d] Yield of **6** after purification by column chromatography. [e] Yield of isolated **6** after two steps (**4**→**5**→**6**).

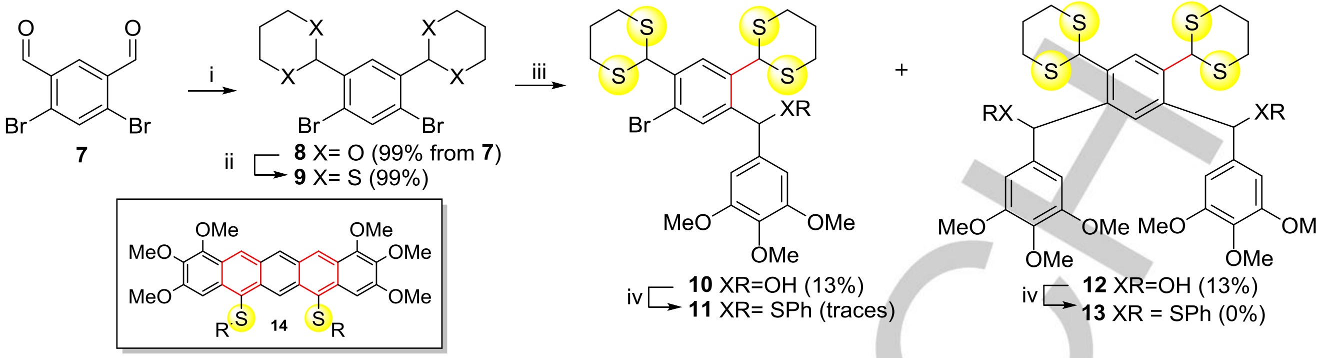

Reaction conditions: i) 1,3-propanediol, *p*-TsOH(cat.), toluene, reflux; ii) 1,3-propanedithiol, I_2, $CHCl_3$, RT, 48h; iii) *n*-BuLi; 3,4,5-trimethoxy-benzaldehyde, THF, -78°C; iv) PhSH, *p*-TsOH, AcOEt, RT

Scheme 2. Synthesis of substrates **10-12** for the double thio-Friedel Crafts/Bradsher cyclization.

Photophysical, electrochemical, thermal and photochemical, properties of mono-RS-(hetero)acenes 6.

Absorption and emission steady state measurements: Optical properties of mono-RS-substituted (hetero)acenes **6a-g** were measured in six solvents (ethanol, tetrahydrofuran, ethyl acetate, cyclohexane, toluene, acetonitrile) (Tables 4-10, see SI).

The absorption spectra of the anthracenes **6a-d**, with identical alkoxy substituents and different SR groups (**6a**-SPh, **6b**-S-2-Naphthyl, **6c**- S-Alkyl, **6d**-S-Benzyl) had the same absorption pattern in the range of 310-425 nm with only two absorption maxima at λ_{maxabs}= 380/400 nm. In case of the anthracene **6e**, absorption spectra in the above solvents exhibited four absorption maxima at λ_{maxabs}= 345/365/380/400 nm, while in case of **6g**, containing four fused rings, only two, low lying maxima at λ_{maxabs}= 345/377 nm in the range of 310-450 nm, were observed. The fluorescence spectra of **6a-f** showed a blue emission in all six different solvents (*vide supra*) with emission maxima in the ranges of 435-457 nm for **6a-d**, 436-440 nm for **6e,** 403-424 nm for **6f** and 385-401 nm for **6g** (Table S4-10, see SI). The Stokes shifts of 59-78 nm for **6a-d** revealed weak interactions between the six solvents and the excited molecules **6a-d** (Tables S4-10, see SI). Absorption and emission bands values for (hetero)acenes **6a-g** in two selected solvents (EtOH and toluene) are summarized in Table 3 (for the remaining four solvents, Tables S4-10, see SI). Emission and absorption spectra for **6a-g** in these solvents are visualized in Fig. 1 and 2. Analysis of these spectra in the above solvents showed neither absorption nor emission solvent effects (Tables S4-10, see SI).

Time-resolved measurements: In addition to the steady state measurements, the time-resolved experiments also were carried out. Table 4 presents the fluorescence lifetimes (τ) of acenes **6a-f** and the fluorescence quantum yields Φ.The highest Φ values of 42.9% (THF) exhibited **6a** with the SPh substituent and **6c** with the $SC_{12}H_{25}$ substituent (32.7%,THF). The compound **6f** showed the lowest quantum yields <1% in all solvents. Lifetimes (τ) of **6a-f** were also measured in the above six solvents (SI) for which the chi-square values χ^2 are given in Table 4. These values judge the quality of the two- or one-component fit between the measured data and the calculated single or multiple exponential decays in the least squares analysis.[71] The value of χ^2 is the sum of squares deviations between the measured and expected values, each divided by squared deviations expected for the number of detected photons. The lifetimes were relatively short in nonpolar solvents, such as cyclohexane (Cy) and toluene. For **6d** and **6f**, two lifetimes, one short (τ_1) and one long (τ_2), were measured (**6d** - τ_2/τ_1= 6; **6f** - τ_2/τ_1= 11, both in Cy). The radiative k_r (Fig. 3) and nonradiative k_{nr} (SI) rate constants for the selected mono-RS-substituted anthracenes **6a**, **6b**, **6c** and **6e** were also calculated from the measured Φ and τ values.[69] The resulting rate constants were then plotted as a function of the normalized polarity parameter E^N_T (Fig.3, SI).The E^N_T values are dimensionless numbers which correspond to scale ranges from 0.000 for TMS (tetrametylsilane) as the least polar solvent to 1.000 for water, the most polar solvent.[72] As shown in Fig. 3, k_r values slightly decrease with the increasing solvent polarity for all mono-RS-substituted anthracenes **6a-c**, **6e**, whereas k_{nr} are almost independent of the kind of solvent (SI).

All mono-RS-substituted anthracenes **6a-g** emitted blue light with the following coordinates (toluene) corresponding to the CIE 1931 color space chromaticity diagram: **6a** (0.153, 0.089), **6b** (0,150, 0.086), **6c** (0.153, 0.076), **6d** (0.168, 0.283), **6e** (0.163, 0.107), **6f** (0.153, 0.034) and **6g** (0.169, 0.004) (Fig. 4).

Cyclic voltammetry: Cyclic voltammetry measurements were carried out in $Bu_4N^+PF_6^-$ (0.1 mol L^{-1})/dichloromethane solution to determine the HOMO and the LUMO energy levels of **6a-c**, **6e** and **6g** (Fig.5). The oxidation potentials of these compounds were located in a similar potential range except of **6e** and **6g** which could be due to a significant change of fused rings structure and their surroundings. The reversible oxidation of the compounds (i.e. **6a**) was accompanied with a subsequent chemical reaction (i.e. **6g**) while the reduction processes proceed towards the molecule decomposition and therefore results in the recorded irreversibile processes. The molecular frontier orbital levels were estimated from the electrochemical analysis using a method described by Sun and Dalton.[73] In order to calculate the absolute energies of LUMO and HOMO, the redox data were standardized to ferrocene/ferrocenium couple which has a calculated absolute energy of -4.8 eV.[74]

10.1002/chem.201903027

Table 3. UV/Vis absorption and fluorescence properties of **6a-g** in EtOH and toluene solutions.

Comp.	EtOH[a]			Toluene[a]		
	λ_{maxabs} [nm]	λ_{maxem} [nm]	υ[b] [nm]	λ_{maxabs} [nm]	λ_{maxem} [nm]	υ[b] [nm]
6a	379, 399	442	63	380, 401	445	65
6b	379, 400	444	65	380, 403	447	67
6c	376, 395	436	60	377, 398	419, 439	62
6d	378, 397	440	62	379, 401	457	78
6e	345, 365, 380, 401	437	72	345, 367, 383, 403	440	73
6f	362, 382	405	23	364, 384	424	40
6g	345, 377	385, 397	40	348, 379	392	44

[a] Absorption and fluorescence spectra recorded in EtOH and toluene solutions (1 x 10^{-5} M), [b] Stokes shift

Table 4. Fluorescence quantum yields and lifetimes of **6a-f** in different solvents.

		Solvent					
		EtOH	CH_3CN	AcOEt	THF	Toluene	Cyclohexane
	E^N_T [(a)]	0.654	0.460	0.228	0.207	0.099	0.006
6a	$\Phi^{(b)}$	33.3	39.2	34.1	42.9	31.5	34.8
	τ [ns]	6.08	7.20	6.29	6.83	5.43	5.17
	$\chi^{2(c)}$	1.14	1.25	1.26	1.11	1.03	1.10
6b	Φ [%]	16.6	15.3	16.3	16.5	18.3	15.6
	τ [ns]	2.24	2.69	2.42	2.63	2.23	2.02
	χ^2	1.01	1.12	1.13	1.07	1.17	1.00
6c	Φ [%]	17.1	22.7	19.7	32.7	23.5	26.4
	τ [ns]	5.27	6.06	5.11	5.77	4.98	4.58
	χ^2	1.12	1.23	1.15	1.08	1.10	1.09
6d	Φ [%]	0.5	2.5	1.9	10.6	3.1	1.8
	τ_1 [ns]	1.00	1.15	1.23	5.78	2.33	1.21
	τ_2 [ns]	6.16	8.04	7.30	9.34	10.08	7.30
	χ^2	1.01	1.36	1.53	1.20	1.56	1.09
6e	Φ [%]	12.9	12.2	13.1	15.0	15.0	13.5
	τ [ns]	2.10	1.97	2.04	2.24	1.94	1.88
	χ^2	1.06	1.10	1.02	1.56	1.10	1.12
6f	Φ [%]	0.10	0.05	0.05	0.16	0.63	1.39
	τ_1 [ns]	0.47	0.71	0.44	0.53	0.23	0.28
	τ_2 [ns]	2.81	3.14	2.36	2.48	2.17	3.19
	χ^2	1.24	1.05	1.08	1.05	1.12	0.89

[a] Normalized polarity parameter[72]; [b[Quantum yields Φ were measured with an integrating sphere in the solvent indicated at μM concetration (1 x 10^{-5} M); [c] χ^2 – CHISQ (chi square).

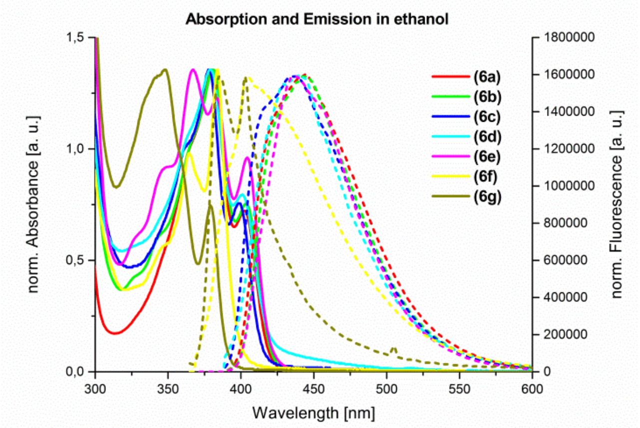

Figure 1. Normalized absorption (solid line) and emission (dotted line) spectra of **6a-g** in EtOH.

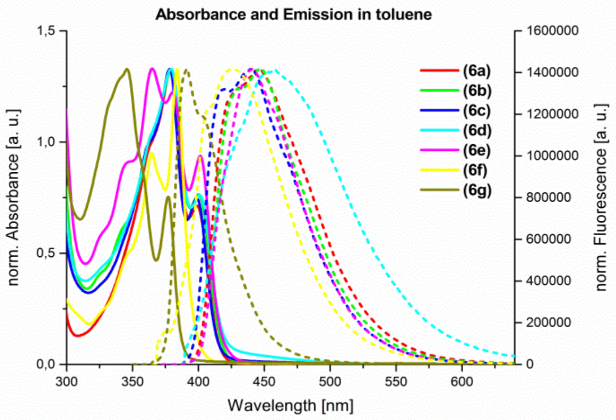

Figure 2. Normalized absorption (solid line) and emission (dotted line) spectra of **6a-g** in toluene.

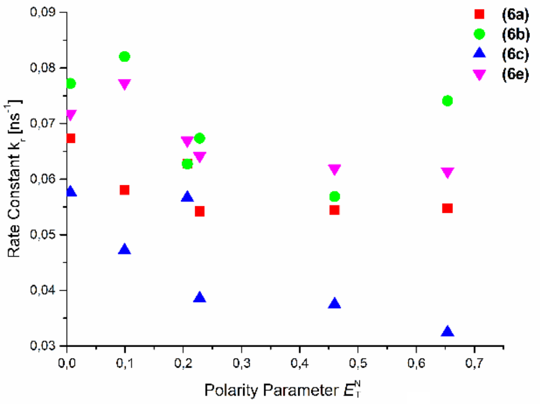

Figure 3. Radiative rate constants plotted against E^N_T (for the non-radiative rate constants see SI).

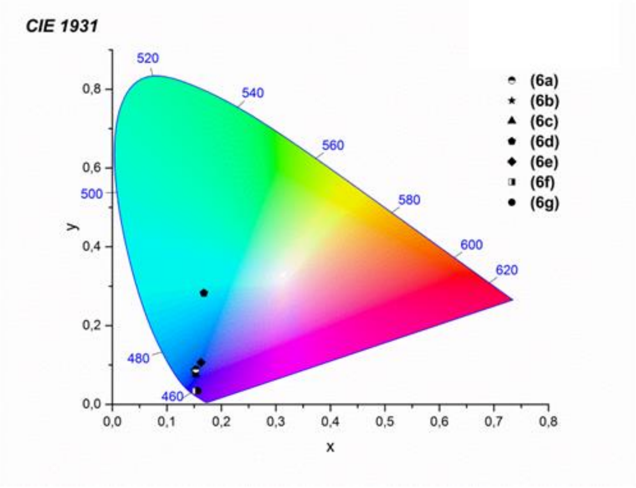

Figure 4. The Commission Internationale de L'Eclairage (CIE) 1931 chromaticity coordinates for mono-RS-substituted anthracenes **6a-g** in toluene solution.

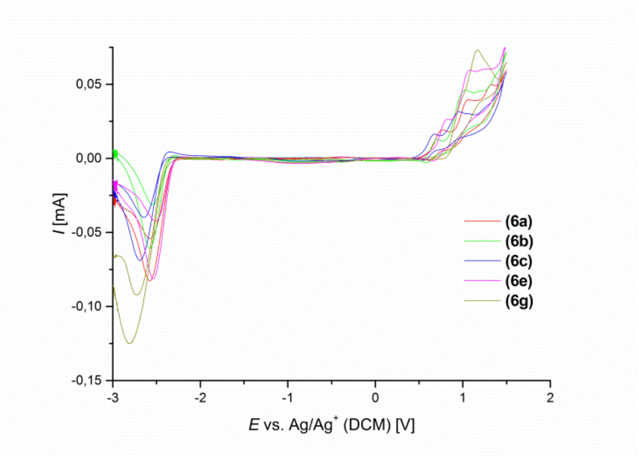

Figure 5. Cyclic voltammograms of selected compounds (concentration of 1 mmol L^{-1}) recorded at a glassy carbon electrode in dichloromethane solution containing 0.1 M $Bu_4N^+PF_6^-$ as supporting electrolyte after subtraction of a blank.

All the measured redox potentials, calculated HOMO/LUMO energy levels and energy gaps Eg values are shown in Table 5.

Thermal properties: Thermal properties of the mono-RS-substituted anthracenes **6** were determined by thermogravimetric analysis (TGA) and differential scanning calorimetry (DSC). Generally, these compounds decomposed in the range of T_d= 331-354 °C, i.e. by average 25 °C (297-331 °C) higher than the reported in literature di-RS-substituted acenes. The highest decomposition temperature (354 °C) was observed for **6g** and the lowest one (331 °C) for **6b**. Solid materials should also exhibit high melting points which depend on chemical structure and a crystal packing pattern. For some mono-RS-**6**, DSC curves showed advantageous melting points: **6f** - T_m= 243 °C and **6g** - T_m= 186 °C, while for others T_m were differentiated: **6b** - T_m=171 °C, **6 l** - T_m= 153 °C[68] , **6c** - T_m= 51 °C. In case of **6a**, three peaks (T_m= 108 °C, 129 °C, 137 °C); **6e**, two peaks

Table 5. Cyclic voltammetry data, HOMO-LUMO levels and energy gaps Eg values of selected acenes **6**.

Cmpd.	E_{ox} (V)	E_{HOMO} (eV)	E_{red} (V)	E_{LUMO} (eV)	E_g (eV)
6a	0.704	-5.485±0.054	-2.562	-2.219±0.059	3.266
6b	0.697	-5.478±0.042	-2.541	-2.240±0.045	3.238
6c	0.653	-5.434±0.027	-2.657	-2.125±0.040	3.309
6e	0.800	-5.581±0.044	-2.500	-2.281±0.047	3.300
6g	0.939	-5.720±0.042	-2.754	-2.028±0.060	3.692

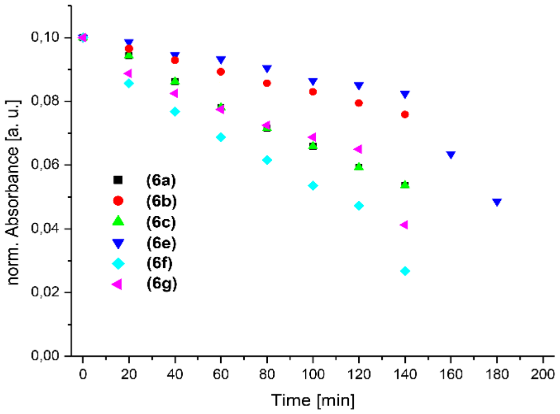

Figure 6. Evolution of the lower energy band absorptions of **6a-c, e-g** in EtOH (10^{-5}M), under the UVP-Pen-ray lamp exposure (254 nm) at room temperature under ambient atmosphere.

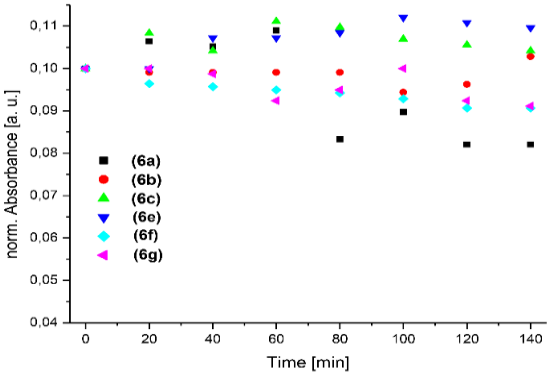

Figure 7. Evolution of the lower energy band absorptions of **6a-c, e-g** in EtOH (10^{-5}M), under the 6 W Tube lamp exposure (365 nm) at room temperature under ambient atmosphere.

(T_m= 164 ^{o}C, 180 ^{o}C) and **6d**, three peaks (T_m= 49 ^{o}C, 90 ^{o}C, 117 ^{o}C) were observed which might indicate formation of different polymorphic structures. For the unfunctionalized di-RS-substituted anthracenes, reported in literature (R = *n*-$C_{12}H_{25}$, *n*-C_3H_7, C_6H_5, 2-Naphthyl),[44] melting points gradually increased from 69 ^{o}C, 109 ^{o}C, 213 ^{o}C to 239 ^{o}C, respectively.

Interestingly, that the RO-disubstituted anthracene (R= *n*-$C_{12}H_{25}$) also melted low, i.e. at 50 ^{o}C,[42] revealing a trend to the lowering of the anthracenes melting points by long alkyl chains (R= *n*-$C_{12}H_{25}$: di-RO, 50 °C[50]; **6c**-RS, 51 ^{o}C; di-RS, 69 °C).[44]

Photochemical stability: The photostability of mono-RS-substituted anthracenes **6a-6g** was investigated by monitoring the 50 % absorbance decay of the lower energy bands. Ethanolic solutions (10^{-5} M) were stored in dark at room temperature under inert and ambient atmosphere and then exposed to the UV light sources of 254 nm (UVP-Hg-Pen-ray lamp, 16.33 mW/cm^2 at distance 1 cm) (Fig. 6) and 365 nm (fluorescent lamp VL-6.LC (6W), 27.4 mW/cm^2 at distance 1 cm) (Fig. 7).The actual irradiation dose (J/cm^2) may be calculated by multiplication of the latter (W/cm^2) by exposure time (sec.). The observed photostability was as follows: for 254 nm under ambient atmosphere: **6b** (249 min.) > **6e** (210 min.) > **6a** (166 min.) > **6g** (153 min.) > **6f** (115 min.) > **6c** (109 min.) and for 254 nm under inert atmosphere: **6b** (519 min.) > **6e** (276 min.) > **6a** (175 min.) > **6c** (115 min.). Generally, at 254 nm under both conditions, the most stable were anthracenes with bulky S-2-Naphthyl groups. The remaining anthracenes **6a**, **6c**, **6f** and **6g** with SPh, S-4-MeO-C_6H_4 and $SC_{12}H_{25}$ groups were stable but significantly less stable than **6b** and **6e** with the 50 % absorbance decay in the range of 109 - 166 min. A comparison of **6b** and **6e** showed another trend to a bit greater stability of sterically crowded, more substituted anthracenes with three methoxy groups versus anthracenes with only one methoxy group (air, 254 nm: 240 min. versus 210 min.), despite the destabilizing electronic effect of methoxy groups (*vide infra*). Significantly bigger differences in the photostability were found for **6b** and **6e** under inert atmosphere (Ar, 254 nm: 519 min. versus 276 min.) Interestingly that stability under air and inert atmosphere at 254 nm for **6a** and **6c** was comparable (166, 109 and 175, 115 nm, respectively). Several isosbestic points, observed in the UV/Vis spectra of **6a-6g** (see SI), indicated the coexistence in solution of the starting materials and their oxidized or degraded products.

Indeed, irradiation of ethanolic solutions of **6a-d**,**f** for 3h in each case (air, 254 nm, irradiation dose 176 J/cm^2) and subsequent HRMS-(+)-APCI analysis of the resulting crude reaction mixtures, confirmed the presence of the starting acenes accompanying with various photo-degradants. The characteristic feature of the latter is maintanance of integrity of all anthracene rings without C-C bonds cleavage and preservation of the longest C-S bonds in most cases due to the C-S bond strengthening in S_1 and T_1 excited states compared to S_0, as in case of **6a** (vide infra). In the mixtures, two main groups of photo-products may be distinguished. They originate from: 1) addition of oxygen to the anthracene rings to initially form endoperoxides or hydroperoxides (not detected) which decompose to cyclic epoxides, phenols or are further oxidized to quinones of 1,2- and/or 1,4-type, 2) oxidation of sulfur atom to sulfoxide and/or oxidation of the anthracene 10-C carbon atom to ketone. In case of **6a** and **6d**, the SBn/OEt and OMe/OEt replacements products due to the solvent used (EtOH), were also detected (see SI).

Stability to photooxidation of compounds **6a**-**6g** upon exposure to the UV light at 365 nm under ambient atmosphere was obviously much higher than the stability upon exposure to the UV light at 254 nm. For instance, the 50% absorbance decay for **6f** was at least 7 times higher at 365 nm than at 254 nm (812 min. at 365 nm versus 115 min. at 254 nm). Further photostability testing under inert atmosphere at 365 nm were not continued due to very long half-lives, significantly exceeding the highest values obtained under ambient conditions.

The various reaction conditions used in literature in the photostability tests and a large number of the variables, make it difficult to compare photostabilities of acenes originating from different literature sources. Thus, our results may be compared with the results obtained under similar photostability testing conditions (244/366 nm, $CHCl_3$) for anthracenedithiophenes having extended anthracene core for which half-lives ($t_{1/2}$) of only 25–58 s have been reported.[11,27] Photostability of 9-AcO-10-(4-AcO-C_6H_4)-substituted anthracene has also been reported on a seconds level at 254 nm in chloroform.[14] The half-life of the significantly substituted 10-benzyloxy-6-bromo-7-formyl-1,2,3-trimethoxy-anthracene, obtained by us earlier, was 40 - 90 times higher than the reported $t_{1/2}$ values for the above anthracenes ($t_{1/2}$= 40 min., 370 nm, chlorobenzene).[59] For a comparison, half-lives ($t_{1/2}$) for the unsubstituted anthracene in aqueous solution, measured as 50% fluorescence abatement, were less than 4 min. at 254 nm and less than 8 min. at 350 nm.[59] In another polar medium H_2O/ACN= 70/30, $t_{1/2}$= 10 min. (the 310–390 nm range, with a maximum intensity at 350 nm).[72] These data were confirmed by Lehto et al.[13] who reported for the parent anthracene a photostability of 3.41-4.50 min. at pH 5.6 and 7.6 (254 nm) under nitrogen, synthetic air or oxygen as purging gases.

As a concluding remark of this subsection, one may state that the obtained half-lives for the most photostable mono-RS-substituted anthracenes **6b** and **6e** (R= 2-Naphthyl) at 254 nm were at least 60-70 times higher under ambient, air atmosphere in polar media than the half-life for the unsubstituted anthracene ($t_{1/2}$= 3.41 min. at pH 7.6).[13] The change of air atmosphere for the inert gas (argon), at the same testing conditions, revealed that **6b** ($t_{1/2}$= 519 min.) was c.a. 130 times more photostable than the unsubstituted anthracene ($t_{1/2}$= 4.09 min. at pH 7.6[13]), i.e. it increased its photoresistance twofold. Similar differences were observed for the half-life of the most photostable RS-acene **6f** at 365 nm (R= 4-MeO-C_6H_4, $t_{1/2}$= 812 min., air), which was about 80-100 times higher than the half-life of the unsubstituted anthracene ($t_{1/2}$= 8-10 min.)[59,72] under air atmosphere in polar media. A further comparison of the photostability of the electron-rich anthracene **6f** ($t_{1/2}$= 812 min.) with electron-rich anthracenedithiophenes possessing extended anthracene core ($t_{1/2}$= 25-40s),[11,27] showed that **6f** is at least 1200-1900 times more stable at 365 nm. Finally, the literature 6-RS-pentacenes[76] under mild photochemical conditions (air, ambient light) revealed $t_{1/2}$= 29 min. for R= SPh and $t_{1/2}$= 43 min. for R= SAc, which is

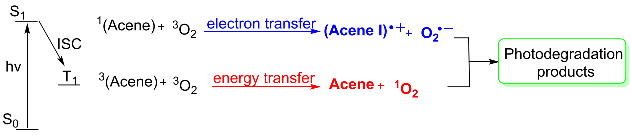

Scheme 3. Two possible mechanistic pathways of the acene photooxidation

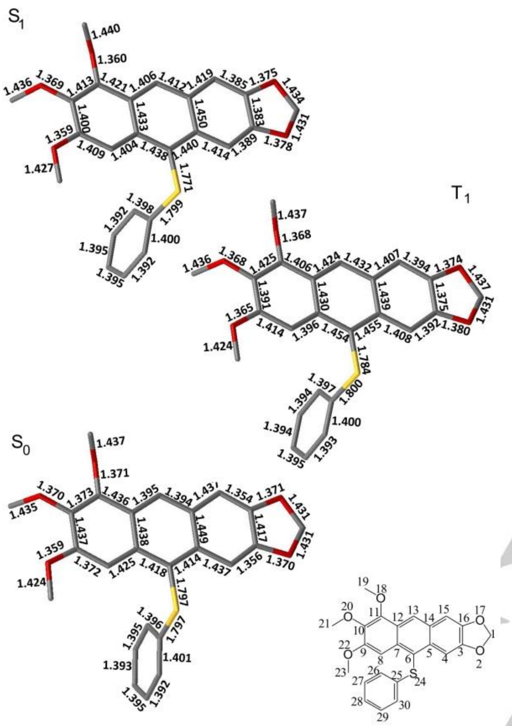

Figure 8. Views of the optimized geometries of S_0, S_1 and T_1 states for **6a**, with the calculated bond distances (in Ångstroms) and its molecular structure with the atomic numbering scheme (H atoms are removed for clarity).

a result of lowering HOMO and LUMO energy levels in the anthracene substituted with a stronger (SAc versus SPh) electron withdrawing group. Interestingly that 6,13-bis-PhS-pentacene lived 40 times longer than 6-PhS-pentacene under the same conditions,[76] most probably due to the substitution of both reactive positions in pentacene that hinders formation of endoperoxide. The described differences in half-lives of acenes are surprisingly large and, indeed, reinforce the need to further study and understand substituent effects in acenes.

The DFT and TD-DFT calculations of electronic structures of mono-RS-6 and explanation of their high photostability.

Generally, there are two mechanisms by which acenes, such as anthracenes **6**, react with oxygen in the presence of light (Scheme 3). In the first, i.e. electron transfer mechanism, the excited singlet acene at the S_1 state is an electron donor to molecular oxygen, which in the ground state is a biradical triplet $^3\Sigma_g$ O_2. The resulting superoxide radical anion and the corresponding acene radical cation are prone to further degradative reactions. In the alternative, i.e. energy transfer mechanism, initiated by the intersystem crossing (ISC) from the S_1 to T_1 state, the triplet acene reacts with the triplet oxygen to give singlet oxygen and acene in the ground state (Scheme 3).

Singlet oxygen is not a radical, but the energy of its molecule is much higher than energy of oxygen in the triplet state. There are two forms of the singlet oxygen: one, ($^1\Delta g$ O_2), has two paired electrons on one orbital π* 2p and the other form, sigma ($^1\Sigma g$ O_2), has one electron on each of the π* 2p orbitals. Energy of the singlet oxygen sigma is higher (157 kJ/mol) than energy of the singlet oxygen delta (94 kJ/mol).

In order to explain the relatively high photostability of mono-RS-acenes **6**, we carried out DFT calculations of electronic structures of compounds **6a** and **6e-6h** in the gas phase, using the gradient corrected three-parameter hybrid functional (B3LYP) with the 6-311++G(d,p) basis set. Full geometry optimizations of these compounds in the ground state (S_0) were performed using the GAUSSIAN 09 quantum chemistry package. Analysis of shape and values of the HOMO/LUMO orbitals was carried out for five mono-RS-acenes derivatives and 6,7-(1,3-methylenedioxa)-anthracene (**6i**), and 6,7-(1,3-methylenedioxa)-9-phenylthio-anthracene (**6j**), treated as the reference compounds (Fig. 8). Moreover, the TD-DFT calculations at the same level of theory, were carried out for **6a** as a representative. First, the electronic excited states in the gas phase were derived, then geometries of the first singlet (S_1) and triplet (T_1) excited states were optimized and finally their excitation energies were calculated. Figure 8 illustrates the optimized geometries of S_0, S_1 and T_1 states for **6a**. In each of these states, the anthracene (**An**) skeleton is essentially planar, and all oxygen atoms and also C-21 carbon atom, are nearly coplanar with the plane formed by this skeleton. In the S_0 state, the deviations of aromatic carbon C3-...-C16 atoms from this plane are relatively insignificant (they lie in the range from -0.028 Å to 0.0123 Å) and increase when passing to the S1 and T1 geometries (the deviations of C atoms from the **An** plane lie in the ranges from -0.0578 Å to 0.0529 Å and from -0.0330 Å to 0.0305 Å, respectively). The dihedral angle between the planes of **An** and phenyl rings is 88.226° in the S_0 state and it decreases to 74.245° and 79.637° for S_1 and T_1 states, respectively. The decrease of this angle is connected with a change of the bond distances between C6 and sulfur atoms, which in the S1 and T1 geometries are shorter by 0.025 Å and 0.013 Å, respectively and thus stronger. The strengthening of the **An**-S bond with the retained length of the Ph-S bond in S_0 and both excited states, is one of the factors responsible for a higher photostability of **6a**. It was also confirmed for other photoproducts derived from **6a-d**,**f** (HRMS-(+)-APCI analysis) which retained the C-S bond untouched upon irradiation (254 nm) at ambient atmosphere (vide supra and SI).This result is rather surprising since in the excited states, the C-S bond as the longest one in **6,** is expected to further lengthen until breaking (true for the formation of 1,4-quinone).The most noticeable change in the bond distances when passing from the S_0 state to the excited states regards to the C-C bonds of the peripherial aromatic rings of the **An** skeleton of **6a** (Fig. 8). In case of the two excited states, the largest differences (i.e. larger than 0.030 Å) with respect to the S_0 state geometry have been found for the C8-C9, C9-C10, C10-C11, C3-C4, C13-C16 and C15-C16 bonds. These differences are c.a. 0.01 Å larger in case of the T1 state and additionally they concern the C5-C6, C6-C7 and C13-C14 bonds, as well. Longer C-C bonds in peripherial rings were responsible for their greater reactivity and formation of ketones (**6b**, **6d**) and 1,2-quinones (**6c**) upon UV irradiation (254 nm) at ambient atmosphere (HRMS-(+)-APCI analysis,SI).

As Figure 9 illustrates, HOMO and LUMO orbitals for each molecule, are mainly located on the anthracene core with exception of **6f**, for which the HOMO orbital is located also on the 4-methoxyphenylthio group.

The geometries of LUMO orbitals of two (hetero)tetracenes **6g** and **6h** are very similar to each other, but the HOMO orbitals vary from one another. In the molecule **6h**, the HOMO, similarly as LUMO, is located mainly on fused aromatic rings, whereas in the molecule **6g**, the HOMO is situated also on the 4-methoxyphenylthio substituent, i.e. just as in **6f**.

Therefore, the LUMOs for these molecules are independent of the type of RS group and consequently a comparison of the LUMO energy values (Fig. 9), calculated for the RS-unsubstituted anthracene **6i** and mono-RS-substituted derivatives **6a**, **6e** and **6j**, showed that (i) the presence of phenylthio substituent in **6j** resulted in the significant decrease of the LUMO energy value from -1.845 eV (in **6i**) to -2.118 eV (stabilizing effect), (ii) introduction of one, electron-donating methoxy group at the 1-anthracene position in **6e,** increased the LUMO energy level to the value of -1.984 eV (destabilizing effect), and (iii) introduction of next two methoxy groups at the positions 2 and 3 in **6a** caused a further increase of this energy up to -1.895 eV (further destabilization). The same trend was also observed for the HOMO energy levels in **6a**, **6e**, **6i** and **6j**. A comparison of the LUMO energy values obtained for **6i** and **6j** (-1.845 eV versus -2.118 eV) resulted in an increase of photostability of the latter due to the presence of the RS substituent. Despite the presence of the destabilizing MeO substituents in **6a** and **6e**, the LUMO energy values calculated for these molecules (-1.895 eV and -1.984 eV, respectively) are still lesser than calculated for **6i** (-1.845 eV) due to the presence of the stabilizing RS group, as well. Indeed, the experimental values of photostability confirmed this relationship (**6a** (3xMeO, PhS): $t_{1/2}$ = 166 min., **6e** (1xMeO, Naphth-S: $t_{1/2}$ = 210 min.).

The HOMO energy levels calculated for compounds **6g** and **6h** are lower, and the values of energy gaps are higher than those calculated for practically all acene derivatives.

In summary of this part, one can conclude that the presence of RS-substituents causes a clear stabilization of mono-RS-acenes due to reduction of their LUMO energies. Thus, the lower LUMO level results in the higher activation energy which prevents the singlet oxygen sensitization and accounts for a reduced rate of photooxidation in these materials due to a possible quenching of the excited state of acenes. (Scheme 4).

The quenching of the acene S_1 state by the $^3\Sigma g$ O_2 in excited acenes, mainly leads to triplet acene and singlet oxygen or to triplet acene and molecular oxygen via an energy transfer reaction (ETR) and the O_2-induced enhanced intersystem crossing (E_{ISC}), respectively.[77,78] A necessary condition for the ETR to occur is the S_1-T_1 energy gap ($\Delta E_{S\text{-}T} = E_{S1\text{-}ET1}$) higher than 94 kJ/mol. In the EISC, the oxygen molecule simply enhances the rate of ISC of the acene molecule and it remains unchanged in this process.[77-79]

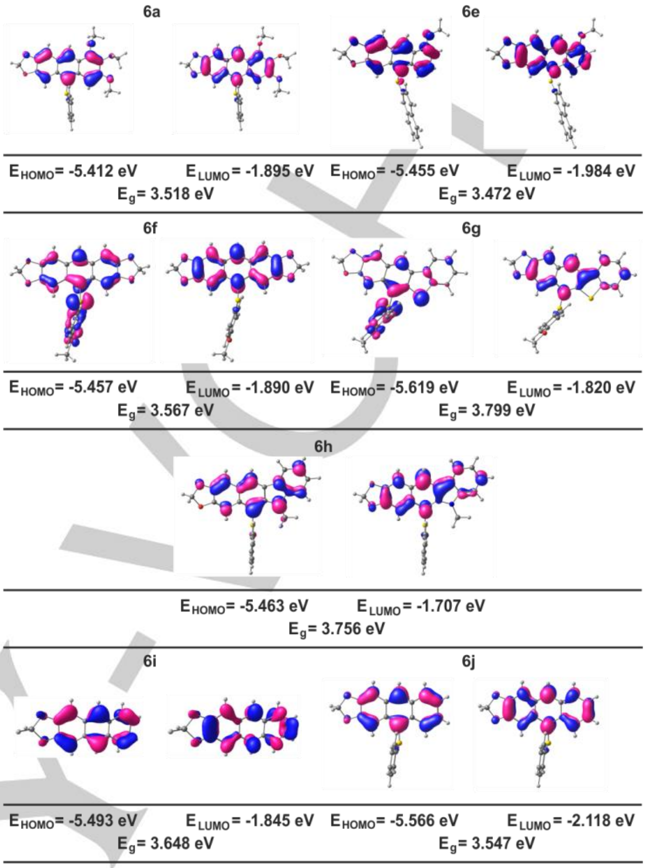

Figure 9. Plots of the HOMO and LUMO orbitals for molecules **6a** and **6e-j** optimized at the DFT theory B3LYP/6-311G(d,p).

In our case, the excitation energies of S_1 and T_1 states (E_{S1} and E_{T1}) calculated for the selected **6a** (due to comparable photostability under ambient and argon atmosphere), are 2.64 eV (255 kJ/mol) and 1.29 eV (124 kJ/mol), respectively. The E_{T1} value lies between the singlet-triplet energy gap ($E_{S\text{-}T}$) for two forms of singlet oxygen, and is higher by only 30 kJ/mol than the energy of the singlet oxygen $^1\Delta_g$ O_2, and by 53 kJ/mol lower than the energy of the singlet oxygen $^1\Sigma_g$ O_2. Thus, the acene **6a** has sufficient energy to generate $^1\Delta_g$ O_2, and too low energy to form $^1\Sigma_g$ O_2.

Taking into account that the S_1-T_1 energy gap calculated for **6a** ($\Delta E_{S\text{-}T}$ = 131 kJ/mol) is larger than 94 kJ/mol, quenching of the S_1 state by ETR and EISC is more likely than photooxidation of **6a** via the electron transfer mechanism for which activation energy is 72 kJ/mol (Scheme 5). The compound **6a** is characterized by a high triplet energy, larger than 94 kJ/mol and relatively low oxidation potential (E_{ox} = 1.390 V versus SCE). So, **6a** can quench $^1\Delta g$ O_2, mainly by the physical process, induced

10.1002/chem.201903027

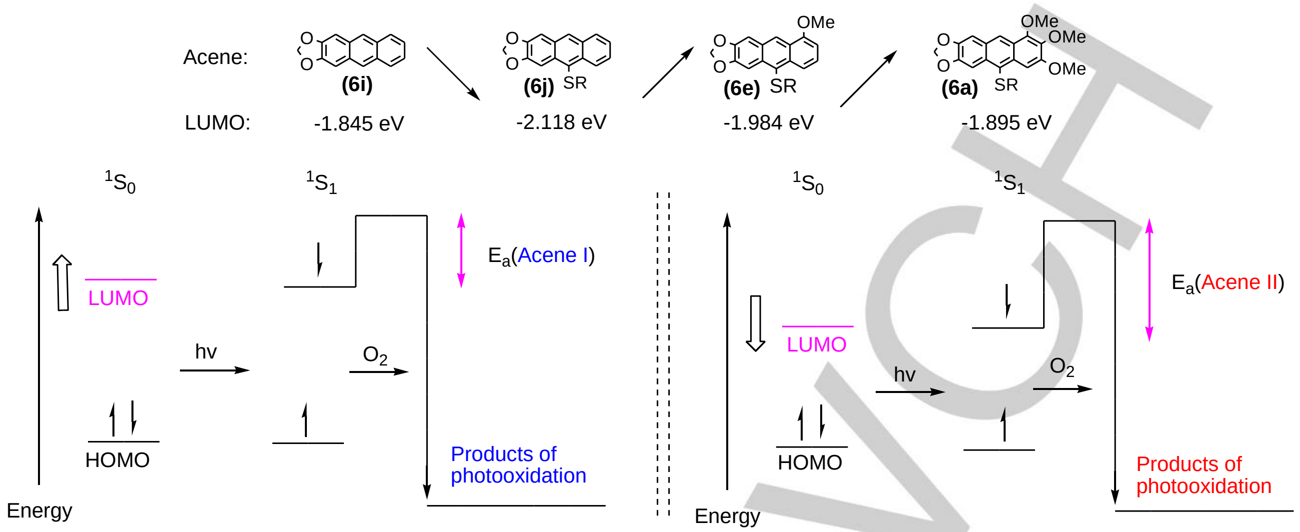

Scheme 4. Two hypothetical situations in photooxidation of acenes **6**: a) increasing the LUMO level of the acene I accounts for a decrease in E_a (activation energy), easier photooxidation and consequently the lower acene photostability (left), b) decreasing the LUMO level of the acene II accounts for the increase in E_a and the higher acene photostability (right).

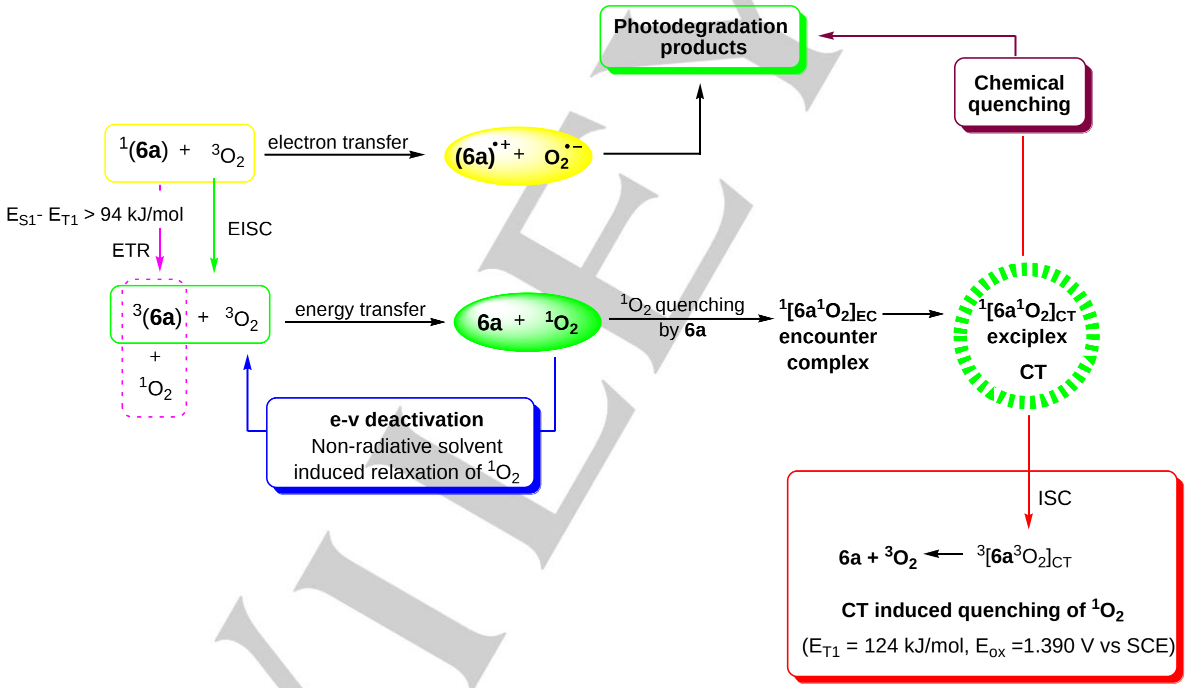

Scheme 5. Photooxidation of the acene **6a** through the energy and electron transfer mechanisms, possible physical and chemical pathways of the non-radiative singlet oxygen $^1\Delta_g$ O_2-deactivation by the acene-**6a** and deactivation of the acene S_1 state by $^3O_2$.

by CT, in which the initially formed singlet encounter complex $^1(\mathbf{6a}^1O_2)_{EC}$ is transformed into a singlet $^1(\mathbf{6a}^1O_2)_{CT}$ exciplex which in turn can decay by the ISC to a triplet CT ground-state $^3(\mathbf{6a}^3O_2)_{CT}$ complex. Finally, it dissociates to **6a** and $^3O_2$. The physical CT process of the $^1\Delta g$ O_2 deactivation may compete with chemical quenching which leads to various photodegradation products. The latter pathway is well documented for the compounds containing electron-rich aromatic systems, amines and sulfides,[77] and so it is also possible in the case of **6a** and other mono-RS-acenes **6**. It is confirmed by the presence of isosbestic points, observed in the UV/Vis spectra of **6**.

Although **6a** does not meet the conditions necessary for the singlet oxygen quenching by the e-v mechanism in its pure form, for which a high oxidation potential is required,[77] the singlet oxygen $^1\Delta_g$ O_2 can interact in solution with hydrogen atoms of the solvent used (ethanol). Thus, $^1\Delta_g$ O_2 is effectively relaxed by energy transfer from electronically excited oxygen to vibrational levels of the solvent (non-radiative, solvent induced relaxation of $^1\Delta_g$ O_2).[77,80] Taking into account that the $^1\Delta_g$ O_2 lifetime in solution depends on the type of solvent, and for the ethanol used by us is relatively short (10 μs),[80] in the case of **6a** and the other mono-RS-**6**, the e-v mechanism is highly probable.

In summary, it is worth emphasizing that the high photostability of mono-RS-acenes **6** under ambient atmosphere is due to the fact that the rates of photooxidation of these materials via both electron and energy transfer mechanisms are reduced to a large extent. The electron transfer from the excited singlet S_1 state of acene to molecular oxygen is hindered mainly by the effective quenching of the acene S_1 state via the ETR and EISC processes. In turn, the most probable mechanisms involving the CT-induced quenching of $^1\Delta_g$ O_2, chemical reactions and non-radiative solvent induced relaxation of $^1\Delta_g$ O_2 also make the energy transfer difficult.

Molecular and crystal structure of 2.

The molecular and crystal structure of the dithioacetal **2**, as well as the molecular Hirshfeld surface of this molecule, have been performed in Fig. 10a-c. For the X-ray crystal structure discussion and the Hirshfeld surface analysis, see SI. Other compounds synthesized in the series **4**, **5** and **6** revealed a weak tendency to crystallization.

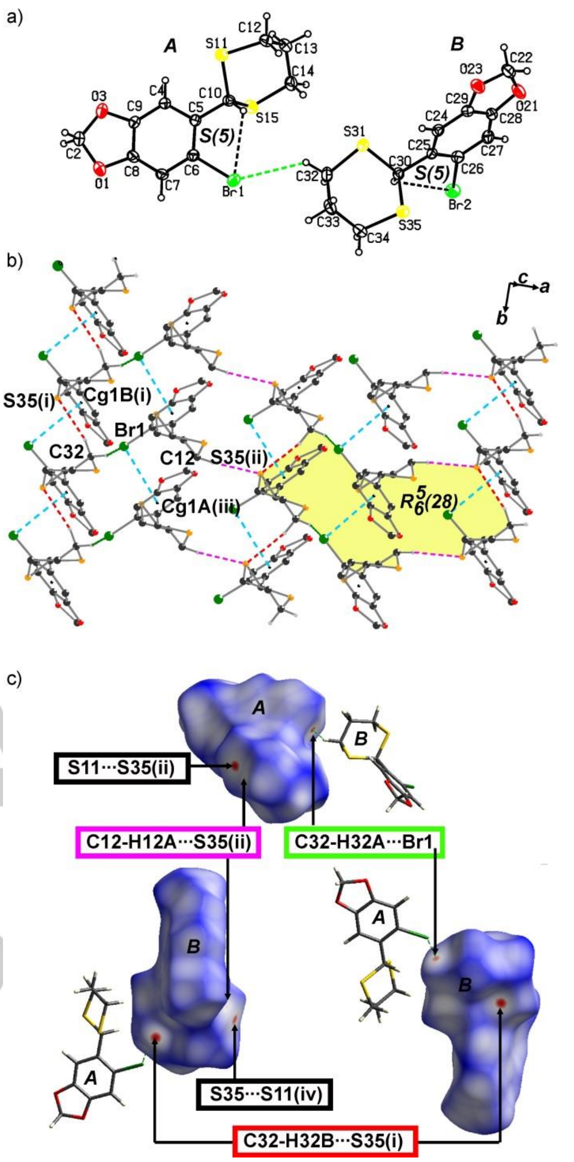

Figure 10. (a) A view of the two symmetry-independent molecules **2** (A and B) with the atom numbering scheme and displacement ellipsoids drawn at the 30% probability level. (b) Part of the crystal structure, showing intermolecular non-covalent interactions: all H atoms not involved in these interactions are omitted for clarity. (c) the Hirshfeld surface of the molecules **2** (A and B) mapped with d_{norm} distance, showing the most dominant interactions in crystal. Symmetry codes: (i) x, -1+y, z; (ii) 1/2+x,1-y,z; (iii) -x, 1- y, -z; (iii) x, 1+y, z; (iv) -1/2+x,1-y, z.

Conclusions

This study presents first examples in which the intriguing and yet underexplored group of small, mono-RS-substituted (hetero)acenes with significant substitution, revealed the highest in their class thermal and photochemical stability at 254 and 365 nm under aerobic and anaerobic conditions. The results were supported by DFT and TD-DFT calculations which revealed the leading role of the RS substituent in the acene stabilization. Both these calculations and analysis of oxidation products (HRMS) showed that one of the factors responsible for enhanced photostability of acenes is strengthening, in the excited S_1 and T_1 states, of the An-S bond which in majority of the analyzed compounds was not cleaved upon UV irradiation (254 nm) at ambient atmosphere. Moreover, the calculations allowed to determine the three possible mechanisms of the singlet oxygen quenching (CT-induced, CR, solvent induced relaxation) and two processes of the acene S_1 state quenching by molecular oxygen $^3O_2$ (ETR, EISC), which may be responsible for the high photostability of acenes **6**. This group of blue emitters was obtained via novel variant of the Friedel-Crafts/Bradsher (thio-F-C/B) reaction involving electrophilic cyclization of unknown *ortho*-1,3-dithioacetalaryl(aryl)methyl thioethers **5**. The new approach complements both original Friedel-Crafts/Bradsher protocol[69] and its oxo-variant,[73,81,87] and constitutes a further contribution to the fundamental knowledge on intramolecular electrophilic aromatic substitution. The protocol is open and enables synthesis of four or more fused (hetero)aromatic rings by utilization of larger *ortho*-bromo aromatic aldehydes which have recently been synthesized in our lab.[81] Moreover, mild reaction conditions give access to larger and highly functionalized fused systems which could not be obtained under harsh conditions of the original Friedel-Crafts/Bradsher reaction. We believe that the findings herein will spur further interest and development of next generation RS-mono-substituted acenes and heteroacenes with significant substitution for practical applications as optoelectronic materials, organic ligands for photocatalysts, stable organocatalysts and other thermally and photochemically resistant materials having additional blue light emission characteristics.

Acknowledgements

The scientific work was financed from the Science Resources (National Science Centre-Poland) 2014-2017 as a research grant 2013/11/B/ST5/01610. DG acknowledges the support from the University of Łódź, through the grant no. B1511100000883.02. Authors kindly thank to Dr A. Bodzioch (CMMS, PAS) for the synthesis of compounds **10**-**12**. Special thanks to Dr. E. Wielgus and Dr I. Bąk-Sypień for the preferential recording the series of ESI, APCI and EI-GC mass.

Keywords: Acenes • Aromatic substitution • Cyclization • Fluorescence • Photo- and thermal stability

[1] N. Sugiyama, M. Iwata, M. Yoshioka, K. Yamada, H. Aoyama, *Bull. Chem. Soc. Jpn.* **1968**, *42*, 1377-1379.

[2] B. Purushothaman, M. Bruzek, S. R. Parkin, A. F. Miller, J. E. Anthony, *Angew. Chem.* **2011**, 123, 7151-7155; *Angew. Chem. Int. Ed.* **2011**, 50, 7013-7017.

[3] J. Zhang, S. Sarrafpour, T. E. Haas, P. Müller, S. W. Thomas, *J. Mater. Chem.* **2012**, *22*, 6182-6189.

[4] W. Fudickar, T. Linker, *J. Am. Chem. Soc*. **2012**, *134*, 15071-15082.

[5] S. S. Zade, N. Zamoshchik, A. R. Reddy, G. Fridman-Marueli, D. Sheberla, M. Bendikov, *J. Am. Chem. Soc.* **2011**, 133, 10803–10816.

[6] M. Usui, Y. Shindo, T. Nishiwaki, K. Anda, M. Hida, *Chem. Lett.* **1990**, *3*, 419-422.

[7] a) J. E. Anthony, *Chem. Rev*. **2006**, *106*, 5028-5048; b) A. R. Murphy, J. M. Frechet, *Chem. Rev*. **2007**, *107*, 1066-1096.

[8] G. W. Breton, X. Vang, *J. Chem. Educ*. **1998**, *75*, 81-82.

[9] S. Ando, J. Nishida, E. Fujiwara, H. Tada, Y. Inoue, S. Tokito, Y. Yamashita, *Chem. Mater.* **2005**, *17*, 1261−1264.

[10] M. Jørgensen, K. Norrman, S. A. Gevorgyan, T. Tromholt, B. Andreasen, F. C. Krebs, *Adv. Mater.* **2012**, *24*, 580–612.

[11] J.-Y. Balandier, F. Quist, N. Sebaihi, C. Niebel, B. Tylleman, P. Boudard, S. Bouzakraoui, V. Lemaur, Cornil, R. Lazzaroni, Y. H. Geerts, S. Stas, *Tetrahedron* **2011**, *67*, 7156- 7161.

[12] L. Zhang, C. Xu, Z. Chen, X. Li, P. Li, *J. Hazard. Mater.* **2010**, *173*, 168-172.

[13] K. M. Lehto, E. Vuorimaa, H. Lemmetyinen, *J. of Photochem. Photobiol. A.* **2000**, *136*, 53–60.

[14] S. A. Azim, H. A. El-Daly, S. A. El-Daly, Kh. A. Abou-Zeid, E. M. Ebeid, J. R. Heldt, *J . Chem. Soc., Faraday Trans*. **1996**, *92*, 2685-2688.

[15] A. B. Prevot, P. Avetta, D. Fabbri, E. Montoneri, A. Morales-Rubio, M. de la Guardia, *Anal. Bioanal. Chem.* **2012**, *404*, 657–664.

[16] M. E. Sigman, S. P. Zingg, R. M. Pagni, J. H. Burns, *Tetrahedron Lett.* **1991**, *32* , 5737-5740.

[17] R. Mondal, R. M. Adhikari, B. K. Shah, D. C. Neckers, *Org. Lett*. **2007**, *9*, 2505-2508.

[18] S. Uttiya, L. Raimondo, M. Campione, L. Miozzo, A. Yassar, M. Moret, E. Fumagalli, A. Borghesi, A. Sassella, *Synth. Met.* **2012**, *161*, 2603–2606.

[19] B. B. Jang, S. H. Lee, Z. H. Kafafi, *Chem. Mater*. **2006**, *18*, 449-457.

[20] L. N. Abusen, Environmental Stability Studies of an Organic Semiconductor. PhD thesis (2013), The University of Manchester, the Faculty of Engineering and Physical Sciences, School of Chemistry.

[21] H. Sun, A. Putta, J. P. Kloster, U. K. Tottempudi, *Chem. Commun*. **2012**, *48*, 12085–12087.

[22] A. B. Lakshminarayana, J. Chang, J. Luo, B. Zheng, K.-W. Huang, C. Chi, *Chem. Commun.* **2015**, *51*, 3604-3607.

[23] I. Kaur, W. Jia, R. P. Kopreski, S. Selvarasah, M. R. Dokmeci, C. Pramanik, N. E. McGruer, G. P. Miller, *J. Am. Chem. Soc*. **2008**, 130, 16274-16286.

[24] T. Mill, B. Y. Mabey, L. A. Baraze, *Chemosphere* **1981**, 10, 1281-1290.

[25] Y. Kawanaka, A. Shimizu, T. Shinada, R. Tanaka, Y. Teki, *J. Am. Chem. Soc*. **2008**, *130*, 16274-16286.

[26] H. Usta, A. Facchetti, T. J. Marks, *J. Am. Chem. Soc*. **2008**, *9*, 8580-8581.

[27] J.-Y. Balandier, N. Sebaihi, P. Boudard, V. Lemaur, F. Quist, C. Niebel, S. Stas, B. Tylleman, R. Lazzaroni, J. Cornil, Y. H. Geerts. *Eur. J. Org. Chem.* **2011**, *17*, 3131-3136.

[28] A. Maliakal, K. Raghavachari, H. Katz, E. Chandross, T. Siegrist, *Chem. Mater*. **2004**, *16*, 4980-4986.

[29] S. S. Palayangoda, R. Mondal, B. K. Shah, D. C. Neckers, *J. Org. Chem.* **2007**, *72*, 6584-6587.

[30] J. E. Anthony, *Angew. Chem. Int. Ed.* **2008**, *47*, 452-483.

[31] a) T. Okamoto, Z. Bao, *J. Am. Chem. Soc.* **2007**, *129*, 10308-10309; b) M. M. Payne, S. R. Parkin, J. E. Anthony, *J. Am. Chem. Soc.* **2005**, *127*, 8028–8029; c) Y. S. Chung, N. Shin, J. Kang, Y. Jo, V. M. Prabhu, S. K. Satija, R. J. Kline, D. M. DeLongchamp, M. F. Toney, M. A. Loth, B. Purushothaman, J. E. Anthony, D. Y. Yoon, *J. Am. Chem. Soc*. **2011**, *133*, 412−415.

[32] Y. Li, Y. Wu, P. Liu, Z. Prostran, S. Gardner, B. S. Ong, *Chem. Mater*. **2007**, *19*, 418-423.

[33] A. A. Gorodetsky, M. Cox, N. J. Tremblay, I. Kymissis, C. Nuckolls, *Chem. Mater*. **2009**, *21*, 4090–4092.

[34] T. Okamoto, M. L. Senatore, M.-M. Liang, A. B. Mallik, M. L. Tang. Z. Bao, *Adv. Mater.* **2007**, *19*, 3381-3384.

[35] K. Ono, H. Totani, T. Hiei, A. Yoshino, K. Saito, K. Eguchi, M. Tomura, J. Nishida, Y. Yamashita, *Tetrahedron* **2007**, *63*, 9699-9704.

[36] a) Z. Chen, P. Müller, T. M. Swager, *Org. Lett.* **2006**, *8,* 273-276; b) H. Moon, R. Zeis, E.-J. Borkent, C. Besnard, A. J. Lovinger, T. Siegrist, C. Kloc, Z. Bao, *J. Am. Chem. Soc*. **2004**, *126*, 15322-15323; c) H. Kunieda, K. Nakamura, D. F. Evans, *J. Am. Chem. Soc.* **1991**, *113*, 1051-1052.

[37] M. M. Payne, J. H. Delcamp, S. R. Parkin, J. E. Anthony, *Org. Lett.* **2004**, *6*, 1609-1612; b) M. A. Wolak, J. S. Melinger, P. A. Lane, L. C. Palilis, C. A. Landis, J. Delcamp, J. E. Anthony, Z. H. Kafafi, *J. Phys. Chem. B* **2006**, *110*, 7928-7937; c) M. A. Wolak, J. S. Melinger, P. A. Lane, L. C. Palilis, C. A. Landis, J. E. Anthony, Z. H. Kafafi, *J. Phys. Chem. B* **2006**, *110*, 10606-10611.

[38] I. Kaur, N. N. Stein, R. P. Kopreski, G. P. Miller, *J. Am. Chem. Soc.* **2009**, 131, 3424-3425.

[39] K. Kobayashi, H. Masu, A. Shuto, K. Yamaguchi, *Chem. Mater*. **2005**, *17*, 6666-6673.

[40] T. Kimoto, K. Tanaka, M. Kawahata, K. Yamaguchi, S. Otsubo, Y. Sakai, Y. Ono, A. Ohno, K. Kobayashi, *J. Org. Chem.* **2011**, *76*, 5018-5025.

[41] Y. Wakayama, R. Hayakawa, T. Chikyow, S. Machida, T. Nakayama, S. Egger, D. G. de Oteyza, H. Dosch, K. Kobayashi, *Nano Lett.* **2008**, *10*, 3273-3277.

[42] K. Kobayashi, R. Shimaoka, M. Kawahata, M. Yamanaka, K. Yamaguchi, *Org. Lett.* **2006**, *8*, 2385-2388.

[43] I. Kaur, M. Jazdzyk, N. N. Stein, P. Prusevich, G. P. Miller, *J. Am. Chem. Soc.* **2010**, *132*, 1261-1263 (see also ref. 2 as a comment to this work).

[44] C. Nerungsi, P.-K. Wanitchang, S. Sahasithiwat, K. Sadorn, T. Kerdcharoen, T.-T. Thongpanchang, *Tetrahedron Lett.* **2010**, *51*, 6392-6395.

[45] A. L. Briseno, Q. Miao, M.-M. Ling, C. Reese, H. Meng, Z. Bao, F. Wudl, *J. Am. Chem. Soc.* **2006**, *128*, 15576-15577.

[46] R. S. Glass, V. V. Jouikov, N. V. Bojkova, *Proc.-Electrochem. Soc.* **2000**, *5-8*, 2000-2015.

[47] P. Charoonniyomporn, S. Thongpanchang, T. Witayakran, Y. Thebtaranonth, K. E. S. Phillips, T. J. Katz, *Tetrahedron Lett.* **2004**, *45*, 457-459.

[48] W. H. Pirkle, J. M. Finn, *J. Org. Chem.* **1983**, *48*, 2779-2780.

[49] K. Radhakrishnam, C.-H. Lin, *Synlett* **2005**, *14*, 2179-2182.

[50] F. D. Saeva, D. T. Breslin, *J. Org. Chem.* **1989**, *54*, 712-714.

[51] M. Node, K. Nishide, K. Ohta, E. A. Fujita, *Tetrahedron Lett.* **1982**, *23*, 689-692.

[52] a) P. G. Del Rosso, M. F. Almassio, M. Bruno, R. O. Garay, *Tetrahedron Lett.* **2010**, *51*, 6730-6733; b) P. H. Lee, Y. Park, S. Park, E. Lee, S. Kim, *J. Org. Chem.* **2011**, *76*, 760-765.

[53] S.-C. Chan, J.-P. Jang, Y.-J. Cherng, *Tetrahedron* **2009**, *65*, 1977-1981.

[54] a) P. R. Christensen, B. O. Patrick, E. Caron, M. O. Wolf, *Angew. Chem. Int. Ed.* **2013**, *52*, 12946-12950; b) L. K. Papernaya, G. M. Panova, E. N. Deryagina, M. G. Voronkov, *Zh. Org. Khim.* **1986**, *22*, 1975-1978.

[55] a) Y. Takikawa, T. Abe, R. Sato, S. Takizawa, *Chem. Lett.* **1980**, *1*, 25-28; b) Y.Takikawa, S. Takizawa, *Nippon Kagaku Kaishi* **1972**, *4*, 761-765.

[56] a) V. Tilika, B. Berzina, O. Neilands, *Latv. PSR Zinat. Akad. Vestis, Kim. Ser.* **1990**, *6*, 738-742; b) L. Engman, J. S. E. Hellberg, *J. Organomet. Chem.* **1985**, *296*, 357-366.

[57] a) M. Tamano, M. Aoyama, J. Koketsu, *Nippon Kagaku Kaishi* **1985**, *4,* 731-734; b) F. A. Davis, J. P. McCauley, S. Chattopadhyay, M. E. Harakal, J. C. Towson, W. H. Watson, I. Tavanaiepour, *J. Am. Chem. Soc.* **1987**, *109*, 3370-3377; c) A. Ishii, Y. Aoki, N. Nokata, *J. Org. Chem.* **2014**, *79*, 7951-7960.

[58] K. C. Majumdar, S. K Chattopadhyay, B. K. Sen, *Indian J. Chem., Sect. B* **1986**, *25B*, 1261-1262.

[59] A. Ishii, S. Kobayashi, Y. Aoki, T. Annaka, N. Nakata, *Heteroatom Chem*. **2014**, *25*, 658-673.

[60] M. Tamano, Y. Nagai, J. Koketsu, *Nippon Kagaku Kaishi* **1987**, *4*, 684-687.

[61] M. V Lakshmikantham, M. Levinson, M. Menachery, M. P. Cava, *J. Org. Chem.* **1986**, *51*, 411-412.

[62] a) C. Friedel, J. M. Crafts, *Compt. Rend.* **1877**, *84*, 1392-1395 & 1450-1454; b) C. K. A Bradsher, *J. Am. Chem. Soc.* **1940**, *62*, 486-488.

[63] a) P. Bałczewski, E. Kowalska, J. Skalik, 10-Thiosubstituted pentahydroxyanthracene derivatives, a method of their preparation and intermediate compounds. EPO appl., No EP-14460003.8, 06.02.2014; EPO patent, No 28896539 2017, 01.02.2017; b) P. Bałczewski, E. Kowalska, J. Skalik, M. Koprowski, K. Owsianik, E. Różycka-Sokołowska, Thio-functionalized acenes and their application, Patent appl., P-4292239, 12.03.2019.

[64] S. Takano, S. Otaki, K. Ogasawa, *Tetrahedron Lett.* **1985**, 26, 1659-1660.

[65] D. C. Harrowven, *Tetrahedron* **1993**, *49*, 9039-9048.

[66] P. Bałczewski, M. Koprowski, A. Bodzioch, B. Marciniak, E. Różycka-Sokołowska, *J. Org. Chem.* **2006**, *71*, 2899-2902.

[67] A. Bodzioch, K. Owsianik, J. Skalik, E. Kowalska, A. Stasiak, E. Różycka-Sokołowska, B. Marciniak, P. Bałczewski, *Synthesis* **2016**, *48*, 3509-3541.

[68] E. Kowalska, P. Bałczewski, *Ultrasonics Sonochem.* **2017**, *34*, 743-753.

[69] B. Valeur, M. N. Berberan-Santos in *Molecular Fluorescence: Principles and Applications, Chapter 3.2*, WILEY-VCH Verlag GmbH & Co. KGaA, Weinheim, **2001**, pp. 42-48.

[70] a) H. Firouzabadi, N. Irabpoor, H. Hazarkhani, *J. Org. Chem.* **2001**, *66*, 7527-7529; b) P. D. Shinde, H. B. Borate, R. D. Wakharkar, *Arkivoc* **2004**, *xiv,* 110-117.

[71] J. R. Lakowicz *Principles of Fluorescence Spectroscopy*, 3rd EditionSpringer Science+Business Media, LLC (corrected at the 4th printing **2010**).

[72] C. Reichardt in *Solvents and Solvent Effects in Organic Chemistry, 3rd, Chapter 7.4,* WILEY-VCH Verlag GmbH & Co. KGaA, Weinheim, **2003**, pp. 411-443.

[73] S. S. Sun, L. R. Dalton in *Introduction to Organic Electronic and Optoelectronic Materials and Devices*, *Ch.3.4.*, CRC Press/Taylor & Francis: Boca Raton, Florida, USA, **2008**.

[74] a) Z. Peng, Z. Bao, M. E. Galvin, *Chem. Mater.* **1998**, *10*, 2086-2090; b) J. L. Bredas, R. Silbey, D. S. Boudreaux, R. R. Chance, *J. Am. Chem. Soc*. **1983**, *105*, 6555-6559.

[75] P. Bałczewski, J. Skalik, P. Uznański, D. Guziejewski, W. Ciesielski, *RSC Adv.* **2015**, *5*, 24700-24704.

[76] J. Y. K. Chan, Synthesis of 6-thiosubstituted pentacenes and study of an unexpected photorearrangement of 6-phenylthiopentacene dimer. Master's Theses and Capstones, **2011**.

[77] C. Schweitzer, R. Schmidt, *Chem. Rev*. **2003**, *103*, 1685-1757.

[78] C. Wu, A. M. Trozzolo, *J. Phys. Chem.* **1979**, *83,* 2823-2826.

[79] a) A. J. McLean, D. J. McGarvey, T. G. Truscott, C. R. Lambed, E. J. Land, *J. Chem. Soc. Faraday Trans*. **1990**, *86*, 3075-3080; b) K.-K. Iu, P. R. Ogilby, *J. Phys. Chem.* **1987**, *91*, 1611-1617.

[80] J. R. Hurst, G. B. Schuster, *J. Am. Chem. Soc*. **1983**, *105*, 5756-5760.

[81] a) P. Bałczewski, A. Bodzioch, J. Skalik, EPO, EP 2583956, A2 20130424, 2013.; b) P. Bałczewski, A. Bodzioch, M. Koprowski, J. Skalik, UPRP, PL 219155, B1 201503312015, 24.07.2014; c) P. Bałczewski, A. Bodzioch, M. Koprowski, UPRP, PL 219334, B1 20150430, 25.08.2014; d) P. Bałczewski, A. Bodzioch, E. Różycka-Sokołowska, B. Marciniak, P. Uznański, *Chem. Eur. J.* **2010**, *16*, 2392-2400; e) A. Bodzioch, B. Marciniak, E. Różycka-Sokołowska, J. K. Jeszka, P. Uznański, S. Kania, J. Kuliński, P. Bałczewski, *Chem. Eur. J.* **2012**, *18*, 4866-4876; *Synfacts - Highlights* in *Curr. Synth. Org. Chem*. **2012**, *8*, 619-625; f) A. Bodzioch, E. Kowalska, J. Skalik, P. Bałczewski, *Chem. Heterocycl. Compd*. **2017**, *53*, 11-20.

FULL PAPER

The role of RS-group: The leading role of one RS-group in high photostabilization (254/365 nm, both in Ar/O_2) of the significantly substituted and thermally stable mono-RS-(hetero)acene fluorophores, obtained via novel thio-Friedel-Crafts/Bradsher cyclization, has been examined and explained by means of DFT and TD-DFT calculations.

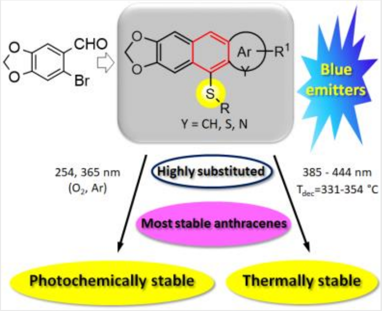

Piotr Bałczewski, Emilia Kowalska, Ewa Różycka-Sokołowska, Joanna Skalik, Krzysztof Owsianik, Marek Koprowski, Bernard Marciniak, Dariusz Guziejewski, Witold Ciesielski*

Page No. – Page No.

Mono-aryl/alkylthio-substituted (Hetero)acenes of Exceptional Thermal and Photochemical Stability via Thio-Friedel Crafts/Bradsher Cyclization Reaction